

Test Environments for 5G Millimeter-Wave Devices

Brett T. Walkenhorst
NSI-MI Technologies
Suwanee, GA 30024
bwalkenhorst@nsi-mi.com

Abstract—As 5G systems are developed and deployed, the RF devices comprising these networks require various types of tests at multiple stages of the design and manufacturing processes. The use of millimeter-wave frequencies and massive MIMO, a combination of technologies intended to ensure sufficient bandwidth and SNR to support massive data throughput, is leading to unprecedented levels of integration of antenna arrays and transceivers. Testing these highly integrated devices is becoming increasingly complex and challenging. In this paper, we investigate various test environments for 5G over-the-air (OTA) testing including far-field, compact range, and near-field chambers. We examine the advantages and disadvantages of each for measuring various over-the-air (OTA) test metrics. This paper offers a high-level trade study by broadly analyzing cost, path loss, and applicability of each environment to different types of OTA tests.

Index Terms—5G, Far-field, Near-field, Compact Range, Millimeter-wave

I. INTRODUCTION

The development of fifth generation (5G) wireless communications technology has been a topic of great interest in the wireless community for several years. The technology promises higher data rates and lower latency than 4G as well as massively scalable networking to support thousands of connections per square kilometer [1].

In order to realize these promises, 5G combines a number of technological innovations including network slicing, massive MIMO, and the use of millimeter-wave spectrum [2]. There are numerous other innovations that have been, and will continue to be, made in support of these major thrusts. In this paper, we are primarily concerned with the combination of massive MIMO and millimeter-wave.

MIMO, which stands for multiple-input multiple-output, is the use of multiple-antenna techniques to achieve higher throughput and/or greater reliability. Though the term initially included only spatial/polarization multiplexing, a broader definition of MIMO has emerged that includes diversity processing and beamforming. The concept of massive MIMO, first introduced in 2010, is the application of MIMO capabilities to large arrays, typically on the order of 100 elements or more [3].

Although massive MIMO can be applied in the lower frequency cellular bands below 6 GHz, termed frequency range 1 (FR1) by 3GPP, spatial multiplexing is likely to be minimal since user equipment (UE) devices will be limited to single antennas or small arrays. In FR1, the base station, called a next generation Node B (gNodeB or gNB) for 5G, will largely employ beamforming with its massive MIMO arrays, as is done in multi-user MIMO (MU-MIMO).

At millimeter-wave frequencies, termed frequency range 2 (FR2) by 3GPP, it becomes possible to mount larger arrays on small UE devices to better enable the full suite of MIMO capabilities. At these frequencies, beamforming is critical. The standard formulation of the Friis transmission equation gives us higher path loss at higher frequencies assuming frequency-independent antenna gain. To overcome this higher path loss at FR2, a high order of beamforming is required to ensure sufficient signal-to-noise ratio (SNR) over a large angular extent to support data rates such as consumers have come to expect. After ensuring sufficient SNR, any remaining degrees of freedom in the MIMO array may be employed in multiplexing. The combination of millimeter-wave with massive MIMO seems a natural fit for achieving good link performance with significantly enhanced throughput.

But this combination, while appealing from the perspective of performance, poses new challenges for the test community. The use of massive arrays of antennas on base stations and UEs necessitates a higher level of integration of antennas and transceivers on devices. 5G equipment is no longer expected to have one or more test point radio frequency (RF) connectors to which test labs can connect their equipment [4]. The input and output from the device may look more like an Ethernet port with digital data in place of RF signals. With the antenna as an integral, inseparable part of the test article, many tests that were previously executed on a benchtop will now have to be conducted in an over-the-air (OTA) configuration.

To perform such OTA testing, we will need to utilize an appropriate chamber. Examining the tradeoffs among the various options for test environments is the focus of the remainder of this paper. In Section II, we look at some of the basic tests that need to be conducted. We discuss 5G device form factors in Section III and millimeter-wave frequency bands for 5G in Section IV. With that context, we then examine several different test environments in Section V, discussing the advantages and disadvantages of each for measuring some of the test metrics discussed in Section II. We summarize our trade study in Section VI.

II. TEST METRICS

Testing wireless devices is done at multiple stages of the life cycle of a device. Initial testing at the R&D stage allows developers to verify their designs meet certain performance requirements, some of which are specific to the vendor. Test environments supporting this stage may look similar to those of other stages, but often require some sort of customization peculiar to the needs of each specific vendor.

A second stage involves conformance testing where independent tests are conducted based on test and

performance specifications established by 3GPP. These specifications become the standard by which devices are validated for operation within the larger wireless ecosystem.

A third stage of testing is conducted during production to ensure mass-produced devices meet certain minimum performance requirements and are free from significant manufacturing defects. These tests may be simpler and faster than conformance tests and are not directly controlled by 3GPP or any other standards body.

While all three types of tests contain some common elements and may often be conducted within the same test environment, because of the commonality of conformance testing among all vendors, we will focus our attention on what is currently known about that type of testing.

Conformance testing may be broken into three different types of tests. Listed in order of increasing complexity, they are: RF, demodulation, and radio resource management (RRM) testing.

A. RF Testing

RF testing includes transmitter and receiver characteristics such as total radiated power (TRP), effective isotropic radiated power (EIRP), effective isotropic sensitivity (EIS), etc. Measuring TRP involves the establishment of a link using a measurement probe, directing the device to lock its beam, then taking spherical measurements to compute the TRP value. For EIRP and EIS, a single measurement is made on the peak of the main beam. The RF measurements are relatively simple in that they require no spatial channel models and no secondary probe.

RF testing may also include out-of-band emissions testing and passive intermodulation (PIM) testing. These tests require very high SNR in order to have confidence in measuring very low emission levels.

B. Demodulation Testing

Demodulation testing adds spatial and/or temporal channel models to assess throughput, error vector magnitude (EVM), and other similar metrics under realistic channel conditions. At a minimum, this requires temporal channel models to emulate, among other things, doppler shift and doppler spread. But the addition of a spatial component of the channel model is more difficult. In [5], two methods are approved for conducting such tests: the multi-probe anechoic chamber (MPAC) and the radiated two-stage (RTS) method.

The MPAC uses multiple probes surrounding the antenna under test (AUT) to synthesize plane-wave conditions within a test zone covering the physical extent of the device. Unfortunately, at millimeter-wave frequencies, the number of probes required for the MPAC can reach into the hundreds, which becomes prohibitively expensive.

The RTS method measures the antenna pattern of an AUT in the first stage of the test, enabled by a special test function within the device. The second stage then combines the measured pattern with the spatial channel model, which is then applied to the signal and transmitted from a single-probe test system. This method currently has no mechanism for handling beam switching, so it is applicable only in scenarios with limited mobility. The advantage of the RTS method is its lower cost compared to the MPAC and the ability to implement demodulation testing in the same test environment used for RF testing.

C. RRM Testing

RRM testing involves the generation of at least two signals emanating from different directions. This can include tests like interference blocking, cell selection, handoff, etc. In this case, it is likely not possible to simplify the test with RTS to use a single probe, since the AUT's behavior for most of these tests must include some type of beam switching. While an MPAC could be used, the cost of implementation may make this infeasible.

One possible solution might include the use of two or more probes, combined with temporal channel models, to approximate the channel conditions that would exist in the real world. The spatial channel model in such an implementation would be overly simplistic, dictated solely by the angular separation of the probes. This simplification could be remedied by using a set of sparsely populated clusters of elements. These clusters could utilize MPAC processing to achieve the correct spatial characteristics and, if necessary, could be made physically mobile to approximate the physical motion of scattering clusters in a mobile scenario. This concept is taking shape within 3GPP under the term simplified sectorized MPAC (SS-MPAC).

III. AUT SIZES

For this analysis, we concern ourselves with two major classes of test articles: UEs and gNodeBs. UEs include handsets, tablets, laptops, and user terminals. For handsets, we assume a form factor no larger than 15 cm; for other UEs, we assume a range from 20 to 60 cm.

For gNodeBs, there may be a variety of form factors depending on vendor, application, and deployment type, ranging from dense urban cells to large rural cells. For our analysis, we will assume these antennas are limited to a range of sizes from 50 cm to 3 m.

IV. FREQUENCIES OF OPERATION

In this paper, we focus our analysis on the millimeter-wave band. While some sources discuss 5G operation as high as 86 GHz, 3GPP currently addresses frequencies from 24.25 to 52.6 GHz [6] while current frequency allocations for initial deployments appear to focus on 28 to 43.5 GHz. We restrict our analysis to this last range of frequencies.

V. TEST ENVIRONMENTS

This section examines the impact of different test environments for conducting the 5G tests described in Section II. In each of the subsections below, we examine a different environment and consider its strengths and weaknesses.

A. Far-field chamber

A far-field chamber offers real-time measurements that achieve far-field conditions, as are typically required for antenna measurements [7]. For RF measurements such as EIRP, EIS, etc., this feature of far-field chambers is very appealing because such quantities are defined as far-field metrics. While demodulation and RRM metrics may be less clear, we still need to create far-field conditions such that the spatio-temporal channel model we want to implement is not inadvertently perturbed by near-field test conditions. For repeatability and fidelity of the test, far-field conditions should be maintained for all OTA tests.

The far-field condition is achieved when the phase taper of a wave emanating from one antenna across the aperture

of another antenna is no larger than $\pi/8$ radians, leading to a far-field distance of

$$R = \frac{2D^2}{\lambda} \quad (1)$$

where D is the size of the aperture and λ is the wavelength.

Using the AUT sizes discussed in Section III and the frequencies in Section IV, we compute range lengths of 4.2 to 6.5 meters for the smallest UEs ($D = 0.15$ m) and 1680 to 2610 meters for the largest gNBs ($D = 3$ m). These range lengths are prohibitively large. While it is possible to design and build such large chambers, the construction and absorber treatment becomes very expensive. Even for the very small UEs ($D = 0.15$ m), the far-field distance is significant, ranging from 4.2 to about 6.5 meters.

Abstracting out the gains of the antennas, we can characterize the free-space path loss as

$$L_p = 20 \log_{10} \left(\frac{4\pi R}{\lambda} \right). \quad (2)$$

Gain-independent path losses for the range lengths computed from (1) vary from -74 to -81.5 dB for small UEs and from -125.9 to -133.5 dB for large gNBs.

We could compute received power and SNR by including transmit power, antenna gains, and noise power, but in this paper, we are primarily concerned with relative path loss across frequency, AUT size, and test environment. But it should be noted that these path losses associated with a traditional far-field chamber are extremely high. For the sake of conserving cost and achieving a higher SNR, it is desirable to find other solutions for testing 5G devices.

B. Quasi-far-field chamber

With the objective of achieving far-field conditions in a smaller chamber, some analysis has shown that it may be possible to use a reduced range length if the radiating aperture is much smaller than the test article [8]. We call the test environment that utilizes this concept a quasi-far-field (QFF) chamber since it does not strictly obey the traditional definition of far-field. While (1) traditionally defines D as the size of the device, the QFF considers D to be only that portion of the device that is expected to be radiating.

3GPP has approved the use of this concept as a valid test environment for 5G UE conformance testing and calls it direct far-field (DFF) [9]. One of the UE models for which the DFF system is applied is a user-equipment (UE) device limited to 15 cm in size with active subarray limited by 5 cm. Under the assumption that the 5 cm aperture determines the far-field distance, a range length of 72.5 cm is sufficient to ensure the subarray experiences no more than 22.5 deg of phase taper at 43.5 GHz when the center of the subarray is aligned with the range axis.

This test environment has the same advantages as the far-field chamber if the assumption about the reduced range length holds. There is a risk with this environment that surface currents on the AUT are not restricted to the physical dimensions of the subarray, which would lead to a larger phase taper than desired. This risk may be mitigated by testing to ensure that, for the device under test, the received power vs range length exhibits a slope similar to that dictated by (2). But the validity of this method is somewhat in question since near-field coupling is dependent on the AUT's current distribution as will be seen in Section V.D. And it requires the ability to translate the AUT along the range axis, which increases overall chamber cost.

Using the 3GPP assumption of a 5 cm aperture for a 15 cm device as a starting point, we compute path loss for each of the AUT sizes assuming the active subarray size is 1/3 the dimension of the overall AUT.

Results will be shown in a later figure, but in comparison to the far-field chamber, the path losses for the quasi-far-field chamber are about 20 dB better. The range lengths are also shorter, but still extremely large for the gNB form factors. The largest form factor requires range lengths of almost 300 meters while the smallest gNodeBs (50 cm) require over 8 meters at 43.5 GHz.

C. Compact range

In addition to the DFF test environment, 3GPP has also approved the use of a compact range, or compact antenna test range (CATR), for 5G testing. In [9], this is referred to as an indirect far-field (IFF) system. The compact range uses a reflector to collimate the beam of a feed antenna to synthesize far-field conditions within a cylindrical area called the quiet zone (QZ) [7]. The compact range has the same advantages as a far-field chamber, but in a much smaller volume. As long as the AUT is kept within the volume of the QZ, it will experience far-field conditions. In contrast to the quasi-far-field chamber, no assumptions about surface currents or the size of an active subarray are necessary. Figure 1 shows an illustration of a CATR for a 50 cm QZ. The QZ is shown as the gray cylinder on the right.

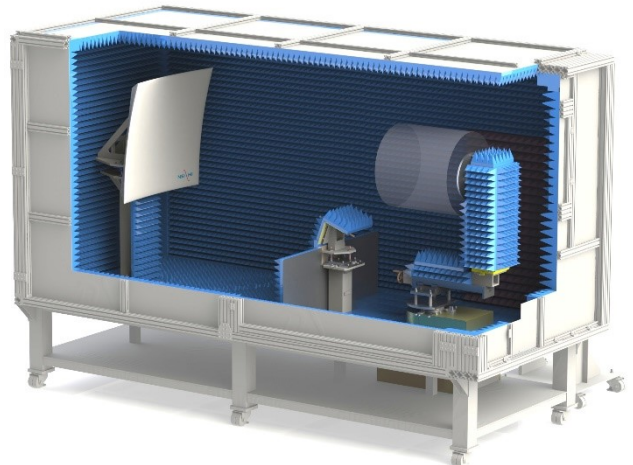


Figure 1. Rendering of a 50 cm QZ CATR

To estimate the path loss in the CATR, we approximate the distance over which spherical spreading occurs as the focal length of the reflector [10]. This is a reasonable approximation for a single offset-fed reflector. It is slightly optimistic compared to the actual path loss experienced by the CATR, but without details of specific reflector designs, this assumption makes generic computation more tractable and is close enough for our purposes.

While the focal length itself is a free parameter in the design, we assume for this analysis that it is equal to twice the diameter of the quiet zone. If we design the CATR to be optimal for the AUT size, we can compute the path loss using (2) where R is the focal length of the reflector.

The path loss of the CATR is lower than that of the QFF, but it is somewhat difficult to say by how much. This is because the slope of the curves is different as illustrated in Section V.E. In an actual system, we would design to meet requirements at all frequencies up to a certain size of AUT. This would fix the chamber size, QZ size, focal length, etc. But in our analysis, we're assuming the chamber exactly meets requirements at each frequency for each size of AUT.

For the CATR, whose focal length is fixed for a given AUT size, the slope of the path loss curves versus frequency is 20 dB per decade. For the QFF system, however, the range length is a function of frequency as well as DUT size. Optimizing at each frequency instead of fixing chamber size at the highest frequency results in a combination of (1) and (2), which makes the slope of the curves 40 dB per decade as indicated in (3).

$$L_p = 20 \log_{10} \left(\frac{\lambda^2}{8\pi D^2} \right) \quad (3)$$

For the 15 cm AUT, the CATR will have an SNR about 4 to 8 dB higher than the QFF. For the 3 m AUT, it is about 30 to 33 dB higher.

D. Near-field chamber

A third test environment approved by 3GPP for 5G testing is a near-field (NF) chamber.

For UE testing, while massive MIMO promises narrow beams, these beams can point in any direction to ensure coverage for any UE orientation. Spherical near-field (SNF) will likely be required for most testing of such devices.

For base stations, cylindrical near-field (CNF) may be an option since these devices are expected to have a limited extent of elevation coverage, typical of terrestrial communications networks.

For simplicity, we'll consider the path loss when the probe is on boresight of the AUT. For both SNF and CNF, we have a probe-to-AUT distance ranging between two values, depending on the geometry of the AUT. For a flat-plate AUT, the distance is equal to the measurement radius. If the AUT has sources extending to the edge of the minimum sphere or minimum cylinder (fictional constructs used in SNF and CNF, assumed to enclose all radiating sources of the AUT) on boresight, the path length is the difference between the measurement radius and the radius of the minimum sphere or cylinder.

A minimum probe-to-AUT distance is typically about 3λ to ensure sufficient decay of evanescent waves. We assume then a NF distance ranging from 3λ to $D/2 + 3\lambda$.

A near-field system has the potential for the lowest loss of any of the test environments discussed. But accurately computing the power density for near-field is more complicated than for the other environments. The approximations made in (2) are probably not valid, depending on the near-field geometry.

For electrically small antennas, we can approximate the near-field coupling as that of a Hertzian dipole, which is the assumption made in [11]. The smallest AUT of 15 cm is 1.4λ at 28 GHz, and the 3 m subarray is 28λ . Most of these AUTs are not electrically small, but even for those that are, the power coupling would increase around distances of less than λ , which is smaller than a near-field chamber would typically use.

In [12], near-field coupling is calculated for a circular aperture with various taper functions. In this case, the models predict that the received power flattens as the distance between antennas decreases to less than $0.1R$ where R is the far-field distance computed in (1). This gives a very different result than the first model. We could approximate our AUT models as circular apertures as this model suggests, but with limited data of actual AUT models for 5G devices, any assumptions would cause problems for the general applicability of our results.

Computing power coupling in the near-field is highly dependent on the geometry and current distribution of the AUT. We can't impose too many detailed assumptions without narrowing the focus of the study, so as a rough approximation, and recognizing the limits of our model, we will use (2) and note that the results may vary significantly from the values presented here. But measured results will almost certainly show the near-field environment to be more favorable in terms of path loss than any of the other test environments.

While path loss is lowest with near-field, this environment has several disadvantages.

1. Phase Recovery

Traditional near-field to far-field (NF-FF) transforms require phase information, so some mechanism must exist for performing phase recovery of the transmitted signal. In traditional antenna testing, this is usually done by directly coupling off the transmitted signal to act as a phase reference. With the level of integration expected for millimeter-wave devices, we will likely not have access to an RF port.

When the AUT is transmitting, directly coupling an RF signal from the AUT is not possible without an RF port. The phase may still be recovered with a separate probe at a fixed position in the AUT's coordinate frame, but this method may lead to poor and/or unpredictable SNR.

When the AUT is receiving, we can easily extract a phase reference, but we won't have access to the RF signal received by the AUT, so we have no complex data against which we can compare our phase reference signal. It may be possible to extract the data using a digital interface, but the IF bandwidths of 5G will make this challenging. Near-field testing is likely not very feasible for RF receive metrics.

2. Transforming Modulated Signals

NF-FF transforms operate on a single frequency. When testing with modulated signals, this single-frequency assumption presents some challenges. The traditional transform may be applied across the band by multi-band filtering to yield patterns at multiple points across the signal spectrum. Or a single pattern approximating the response at the carrier may be obtained by collapsing the spectrum through tightly synchronized temporal correlation with a known signal or a referenced copy of the modulated signal. But all these methods make certain assumptions that will ultimately introduce some error in the final result.

3. Real-Time Links

Finally, near-field requires a complete 2-D raster of data to be acquired in order to transform patterns to the far-field. So, any tests requiring the use of real-time links, such as demodulation and RRM testing, are unlikely to be successful in a near-field test environment.

E. Summary of Path Loss Estimates

Figure 2 shows a summary of path loss vs AUT size for 28 and 43.5 GHz. These values follow from the discussions above. Note the slope of 40 dB per decade for the far-field and quasi-far-field curves and 20 dB per decade for CATR and near-field. The dotted line at the bottom corresponds to a probe-to-AUT distance of 3λ while the other near-field curves show path loss for the larger value of $D/2 + 3\lambda$.

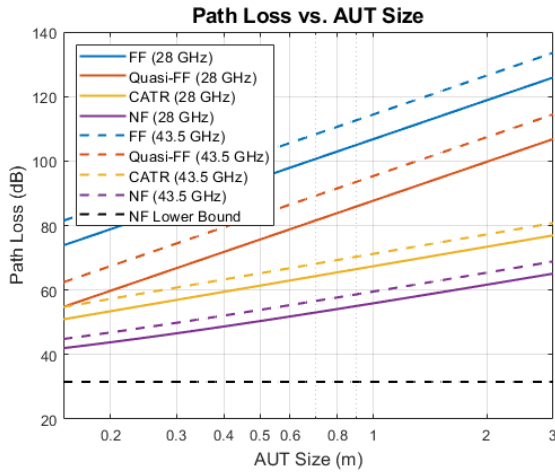


Figure 2. Path loss vs. AUT size

VI. SUMMARY

Different test environments offer different advantages and disadvantages for various types of tests. We summarize these briefly here. Though path loss varies widely among them, except for the traditional far-field chamber, all are potential candidates for various types of 5G OTA testing.

The NF method offers the highest SNR, but is mostly limited in its applicability to RF transmit testing. This is due to several factors including: 1) the need to perform phase recovery over the air; 2) a lack of real-time response, making measurements involving real-time links with modulated signals infeasible; and 3) the assumption of a single frequency when performing NF-FF transforms, which introduces error when making measurements with modulated signals.

The CATR's path loss is not as good as NF but offers almost complete applicability across all types of tests. One exception to this is RRM testing, where the single-probe, single-angle of arrival nature of a CATR prevents us from directly generating two far-field signals at two distinct angles of arrival. This could be remedied with a more complicated feed structure at the loss of some polarization purity. But the resultant spatial separation of signals would be limited in angular extent. Another option would be to pair the CATR with a secondary probe that uses the QFF assumptions as a hybrid solution.

The QFF environment has the highest path loss of the three, but the broadest applicability across test metrics. But its applicability is extremely limited across AUTs. Even for the smallest UEs, it is only applicable under the assumption that a single subarray is transmitting. Other disadvantages include the assumption of far-field conditions at a much smaller range length, which may not always hold, and its still significant range lengths for large AUT sizes, which can be almost 300 meters for the largest AUTs at the highest frequencies. Even the smallest gNBs of 50 cm require range lengths of over 8 m. These chamber sizes and associated costs give a practical limit to the QFF's applicability to larger test articles.

Table 1 summarizes the applicability of the various test environments to the different types of tests and AUT sizes. Colors indicate quality of the solution in terms of SNR, utility, cost, etc.

Table 1. High-Level Summary of Applicability and Quality of 5G Test Environments

	AUT Size	FF	QFF	CATR	NF
RF Testing	Small UEs	Yellow	Green	Green	Tx only
	Large UEs	Red	Yellow	Green	Tx only
	gNodeBs	Red	Red	Green	Tx only
Demod Testing	Small UEs	Yellow	Green	Green	Red
	Large UEs	Red	Yellow	Green	Red
	gNodeBs	Red	Red	Green	Red
RRM Testing	Small UEs	Yellow	Green	Yellow	Red
	Large UEs	Red	Yellow	Yellow	Red
	gNodeBs	Red	Red	Yellow	Red

As shown in the table, FF is not a good choice due to SNR and size and cost of the chamber. NF is limited in its applicability, only working for Tx RF tests. The QFF is a decent solution for small UE testing, if its assumption about surface currents holds and the AUT activates only one subarray. For larger UEs and gNodeBs, QFF becomes increasingly poor due to low SNR and large chamber cost.

The CATR offers the most robust solution for different types of tests and multiple device sizes. It is slightly more expensive than QFF for small UEs due to the cost of manufacturing the reflector. Its major limitation is in RRM testing.

ACKNOWLEDGMENT

The author is indebted to Marion Baggett of NSI-MI Technologies for helpful discussions on near-field power coupling and to the EuCAP reviewers for their thoughtful feedback.

REFERENCES

- [1] *Minimum requirements related to technical performance for IMT-2020 radio interface(s)*, ITU-R M, Document 5/40-E, Feb 2017.
- [2] E. Hossain, M. Hasan, "5G cellular: key enabling technologies and research challenges", *IEEE Instrumentation and Measurement Magazine*, vol. 18, no. 3, pp 11-21, May 2015.
- [3] T.L. Marzetta, "Noncooperative cellular wireless with unlimited numbers of base station antennas", *IEEE Trans. Wireless Commun.*, vol. 9, no. 11, pp 3590-3600, Nov 2010.
- [4] M. Rumney, "Testing 5G: time to throw away the cables", *Microwave Journal*, Nov 2016.
- [5] *Verification of radiated multi-antenna reception performance of user equipment (UE)*, 3GPP TR 37.977, V14.6.0, Jun 2018.
- [6] *User Equipment (UE) radio transmission and reception; Part 1: Range 1 Standalone*, 3GPP TS 38.101-1, V15.3.0, Sep 2018.
- [7] *IEEE standard test procedures for antennas*, IEEE 149-1979, 1979.
- [8] R4-1700531 "Far field distance determination based on power measurements", Rohde & Schwarz, 3GPP TSG-RAN WG4 Meeting #82.
- [9] *Study on test methods for New Radio*, 3GPP TR 38.810 V2.6.0, Sep 2018.
- [10] M. Baggett, D. Hess, "Power handling considerations in a compact range", *AMTA Symposium*, Oct 2013.
- [11] *Near field channel model*, IEEE P802.15-04/0417r2, Oct 2004.
- [12] *Study on the electromagnetic radiated field in fixed radio systems for environmental issues*, ETSI TR 102 457 V1.1.1, Aug 2006.